URSI GASS 2020, Rome, Italy, 29 August - 5 September 2020

Modellization and Control of Spurious Frequency Generation due to Rayleigh Backscattering in Low-Frequency-Radio over Fiber Systems for Radioastronomic Application

Andrea Giovannini* (1), Jacopo Nanni (1), Simone Rusticelli(2),
Randall Wayth(3), Enrico Lenzi (4), Federico Perini(2), Jader Monari(2), and Giovanni Tartarini(1)
(1) DEI-University of Bologna, Viale del Risorgimento 2, 40136 Bologna, Italy
(2) Institute of Radio Astronomy, National Institute for Astrophysics, Via Fiorentina 3513, 40059 Medicina (BO), Italy
(3) Curtin University, Bentley Western Australia, 6102
(4) Protech S.a.S, Via dei Pini 21, 31033 Castelfranco Veneto (TV), Italy

Abstract

Optical links based on the Radio over Fiber (RoF) Technology are, and are going to be, utilized within the antenna downlinks of important Radioastronomic facilities. In this context, the presence of spurious frequency terms has been observed despite the relatively low power levels of the transmitted of RF signals. The present work gives the theoretical explanation of the onset of these nonlinearities, and rigorously demonstrates an effective countermeasure to the undesired phenomenon.

Keywords: Radio over Fiber, Radioastronomy, Rayleigh Backscattering.

1 Introduction

The Radio over Fiber (RoF) technology has been widely utilized for the distribution of mobile signals in non-line-of-sight scenarios or in user-dense areas. Many other applications take advantage of the attractive features of RoF, including important Radio Astronomic plants, where the low attenuation and large passband offered by the fiber channel give the possibility to realize antenna downlinks of high reliability [1]. Within this context, the Square Kilometer Array (SKA) international effort represents an important example. Indeed, within the SKA1-LOW project, around 130,000 RoF systems will be deployed in Australia, each one carrying the sky signals collected by a receiving antenna in the bandwidth $[50{,}350]MHz$ [2].

In this scenario, an important aspect to be considered is the reception of Radio Frequency Interfering (RFI) tones which have to be regarded as known sources that cannot be avoided. The power level P_{RF} of these RFI tones at the input of the RoF link can be considered to be low ($P_{RF} < 20dBm$) if compared to the typical values generating distortion in RoF telecommunications systems [3][4]. Nevertheless, the unexpected presence of less predictable spurious frequency terms has been observed at the receiver end of RoF links, when signals emulating RFI tones were modulating the RoF Transmitter (Tx). The problem stems from the coherent interaction of the propagating signal with a multitude of attenuated and delayed copies of itself generated by Rayleigh Backscattering (RB) [5]. A solution to the present problem has then been proposed, which applies a technique previously utilized to counterbalance the noise induced by RB [6] [7], consisting in the additional introduction of a modulating (*dithering*) tone in input to the RoF Tx [5] [8]. This work presents a detailed model giving a rigorous explanation of the global phenomenon. After its experimental validation, the simulation tool will be utilized to analyze the effects of the introduction of the *dithering* tone, giving important information on practical aspects of the proposed countermeasure.

2 Theoretical Model Developed

Considering initially a laser modulated by a single tone, the main component of field propagating in the single mode fiber, assumed to be linearly polarized, is represented as:

$$E_{in}(t,z) = E_0\{1 + [m\cos(\omega_{RF}(t-\tau_z))] + a_2[\dots]^2 + a_3[\dots]^3\}^{1/2} \cdot e^{-j\beta z} e^{-\frac{\alpha}{2}z} \cdot e^{jM\sin(\omega_{RF}(t-\tau_z))} e^{j\varphi(t-\tau_z)} e^{-j\omega_0(t-\tau_z)} \quad (1)$$

Where E_0 is the amplitude of the unmodulated laser field, while ω_0 and ω_{RF} are respectively the angular frequencies of optical carrier and RF modulating tone. The quantity $m = I_{RF}/(I_{bias} - I_{th})$ is the Intensity Modulation (IM) index, where I_{RF} is the amplitude of the modulating tone $i_{RF}(t) = I_{RF}cos(\omega_{RF}t)$, and I_{bias} , I_{th} are respectively the bias and threshold currents of the laser source. Moreover, $M = K(f_{RF})I_{RF}/f_{RF}$, is the optical phase modulation (PM) index related to the chirp effect of the laser [9], where $K(f_{RF})$ is the adiabatic chirp coefficient at frequency $f_{RF} = \omega_{RF}/(2\pi)$. Moreover, $\varphi(t)$ is the laser phase noise, and $\tau_z = z/v_g$ is the group delay of the fiber mode, where v_g is its group velocity. Laser response nonlinearities are accounted by a_2 and a_3 ($[\dots]$ $[m\cos(\omega_{RF}(t-\tau_z))]$). Finally, β and α are respectively the propagation and attenuation constants. The field backscattered by Rayleigh effect at fiber input (see Fig.1) is given by:

$$E_{BS}(t, z=0) = \int_0^L E_{in}(t-2\tau_z)\rho(z)dz \quad (2)$$

which is the sum of delayed replicas of the propagating field, each weighted by a reflection coefficient $\rho(z)$ [10].

In Eq. (2), L denotes the fiber length, while τ_z is multiplied by a factor of two to account for the field travelling back to the fiber input section. The $\rho(z)$ delta correlated zero-mean circular complex Gaussian random variables, i.e.:

$$\langle \rho(z_1)\rho^*(z_2)\rangle = 2\sigma^2\,\delta(z_1 - z_2) \tag{3}$$

With $\langle\cdot\rangle$ denoting the ensemble average and σ^2 being the variance of both the real and imaginary parts of ρ. The total field at fiber output end $z = L$ is given by:

$$E(t,L) = E_{in}(t,L) + E_{BS}(t,L) \tag{4}$$

where $E_{BS}(t,L)$ is given by an expression analogous to the one given in (2) save for the fact that the field $E_{in}(t-2\tau_z)$inside the integral operator is substituted by $E_{in}(t-2\tau_z-\tau_L)$ with $\tau_L = L/v_g$. The current detected by the photodiode at the receiving end is then:

$$\begin{aligned} i_{out}(t) &= \mathcal{R}\,|E(t,L)|^2 \approx \mathcal{R}|E_{in}(t,L)|^2 + \\ &+2\Re\mathrm{e}\{\mathcal{R}E_{in}(t,L)E_{BS}^*(t,L)\} = i_s(t) + i_{s,BS}(t) \end{aligned} \tag{5}$$

Where $\mathcal{R}$ is the Responsivity of the photodiode, and where the term $|E_{BS}(t,L)|^2$ has not been included since it is negligible with respect to the other terms. The first term at the second side of Eq. (5) can be straightforwardly derived from Eq. (1) and contains the DC and RF received photocurrents in case of absence of RBS. The second term contains instead the spurious terms generated at frequencies multiples of ω_{RF} by the coherent interaction between the propagating and the backscattered field.

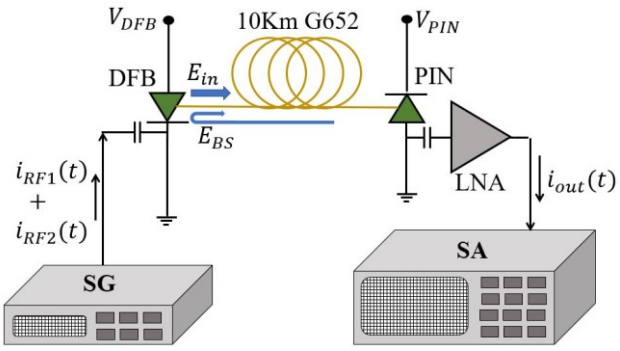

Figure 1. Setup utilized in the experiments. The fields $\boldsymbol{E_{in}}$ and $\boldsymbol{E_{BS}}$ are explicitly indicated for reference purpose.

Exploiting the property (3), the autocorrelation function $R_{out}(\xi)$ of $i_{out}(t)$, can be shown to be expressed as:

$$R_{out}(\xi) = R_s(\xi) + R_{s,BS}(\xi) \tag{6}$$

Where $R_{s,BS}(\xi)$, given by:

$$R_{s,BS}(\xi) = \lim_{T\to\infty}\frac{1}{T}\int_{-\frac{T}{2}}^{\frac{T}{2}}\langle i_{s,BS}(t)\big[i_{s,BS}(t-\xi)\big]^*\rangle dt \tag{7}$$

is the autocorrelation function of $i_{s,BS}(t)$, and where $R_{out}(\xi)$ and $R_s(\xi)$ (the last of which is the autocorrelation function of $i_s(t)$) present a similar form as (7). The final spectrum of $i_{out}(t)$ is given by the sum of the Fourier Transforms $S_s(f) = \mathfrak{F}\{R_s(\xi)\}$ and $S_{s,BS}(f) = \mathfrak{F}\{R_{s,BS}(\xi)\}$. The first of the two can be straightforwardly computed, and results as formed by spectral lines (Dirac distributions) located at DC, at the modulating frequency f_{RF}, and at the multiple frequencies $2f_{RF}$ and $3f_{RF}$, whose presence is related to the quantities a_2 and a_3 of Eq. (1). To compute the second Fourier Transform, it is necessary to first determine $R_{s,BS}(\xi)$. Putting $\Delta\varphi_L(t,z) = \varphi(t-\tau_L) - \varphi(t-\tau_L-\tau_z)$, it is possible to write [7]:

$$\langle e^{j[\Delta\varphi_L(t,z)-\Delta\varphi_L(t-\xi,z)]}\rangle = e^{-\Delta\omega|\xi|}, \quad |\xi| \le 2\tau_z \tag{8a}$$

$$\langle e^{j[\Delta\varphi_L(t,z)-\Delta\varphi_L(t-\xi,z)]}\rangle = e^{-2\Delta\omega\tau_z}, \quad |\xi| > 2\tau_z \tag{8b}$$

where $\Delta\omega$ is the linewidth of the optical field in terms of angular frequency, for which [11] a dependence on the optical PM index M has been assumed. Exploiting (8a,b), after a lengthy but direct derivation, which utilizes again Eq. (3), and assumes without loss of generality that the IM index m is negligibly small, it results:

$$\begin{aligned} R_{s,BS}(\xi) \approx \sum_{p=-\infty}^{+\infty} 2\Re\Bigg\{\Bigg[\int_0^{\frac{v_g|\xi|}{2}} g_p(z)\,e^{-2\Delta\omega\tau_z}dz + \\ + \int_{\frac{v_g|\xi|}{2}}^{L} g_p(z)\,dz\,e^{-\Delta\omega|\xi|}\Bigg]e^{jp\omega\xi}\Bigg\}|E_0|^4 \\ = \sum_{p=-\infty}^{+\infty}\left(A_p + B_p e^{-\Delta\omega|\xi|}\right)cos(p\omega\xi) \end{aligned} \tag{9}$$

where $g_p(z) = |\rho(z)|^2 {J_p}^2(2M\,sin(\omega\tau_z/2))e^{-2\alpha z}$. The expressions of the terms A_p and B_p can directly obtained from the second side of (9). For a given value of p each one of the two consists in an average over z of ${J_p}^2(2M\,sin(\omega\tau_z/2))$, weighted by various z −dependent coefficients. The resulting spectrum is then given by

$$\begin{aligned} S_{s,BS}(f) = \sum_{p=-\infty}^{+\infty}\Bigg[A_p\delta(f-pf_{RF}) + \\ + 2B_p\frac{\Delta\omega}{\Delta\omega^2 + \big(2\pi(f-pf_{RF})\big)^2}\Bigg] \end{aligned} \tag{10}$$

which is a series of Dirac deltas and Lorentzian shaped curves centered in integer multiples of the tone frequency. Following an analogous reasoning, if the laser is modulated by two sinusoidal tones $I_{RF1}\,cos(\omega_{RF1}t)$ and $I_{RF2}\,cos(\omega_{RF2}t)$, it is again lengthy but straightforward to obtain

$$S_{s,BS}(f) = \sum_{p,q=-\infty}^{+\infty} \left[A_{pq}\delta(f - f_{pq}) + \frac{2B_{pq}\Delta\omega}{\Delta\omega^2 + \left(2\pi(f - f_{pq})\right)^2} \right] \quad (11)$$

where $f_{pq} = pf_{RF1} + qf_{RF2}$, and where the terms A_{pq} and B_{pq} consist in this case in an average over z of the product ${J_p}^2(:){J_q}^2(:)$ with $:= 2M_i\, sin(\omega_{RFi}\tau_z/2), i = 1,2$ weighted by various $z-$ dependent coefficients, with $M_i = K(f_{RFi})I_{RFi}/f_{RFi}$ .The presented model can be directly extended to the case when a higher number of sinusoidal tones is initially modulating the laser source.

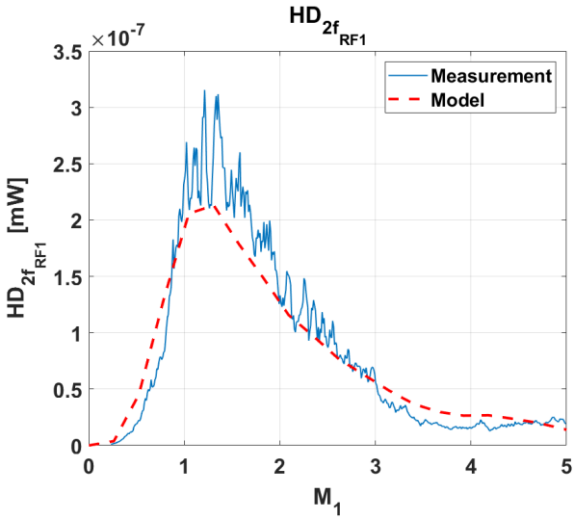

Figure 2. Measured and simulated behaviors of the power generated at frequency $2f_{RF1}$=120MHz when two tones modulate the optical carrier, versus M_1. See text for details.

3 Experimental Results and discussion

The setup utilized for the experimental analysis is reported in Fig. 1. Through a Signal Generator (SG) the modulating signal, consisting, without loss of generality, of two RF tones, is sent to a DFB Laser, which exhibits an adiabatic chirp coefficient ranging from $K = 460\, MHz/mA$ for $f_{RF} = 10KHz$ to $K = 220\, MHz/mA$ for $f_{RF} = 75MHz$. The modulated signal is sent through a fiber span of length $L = 10km$ and reaches a PIN photodetector, followed by a Low Noise Amplifier (LNA) which is in turn connected to an RF Spectrum Analyzer (SA).

3.1 RB-induced distortion terms

Fig. 2 refers to the case of two modulating tones, with frequencies $f_{RF1} = 60MHz$ and $f_{RF2} = 75MHz$, and reports the behavior of the power at the frequency $2f_{RF1}$=120MHz ($HD_{2f_{RF1}}$) when the value of the current amplitude I_{RF1}, which is maintained equal to I_{RF2}, is changed between $0mA$ and $1.36mA$. This corresponds to a input RF power $P_{RF} \in [0, 0.05]mW$. The quantity reported in abscissa is the PM index $M_1 = K(f_{RF1})I_{RF1}/f_{RF1}$, with $K(f_{RF1}) = 220\frac{MHz}{mA}$. It can be appreciated the very good agreement between experimental and theoretical values of the represented quantities, which confirms the correctness of the proposed model. Fig. 3 reports the behavior of $HD_{2f_{RF1}}$ when the currents I_{RF1} and I_{RF2} are changed independently. It can be appreciated that for an assigned value of I_{RF2} (i.e. of M_1), an increase on the value of I_{RF2} (i.e. of M_2), progressively determines a reduction of $HD_{2f_{RF1}}$. This aspect will be developed in the next subsection, to introduce a countermeasure to the described onset of undesired spurious frequency terms.

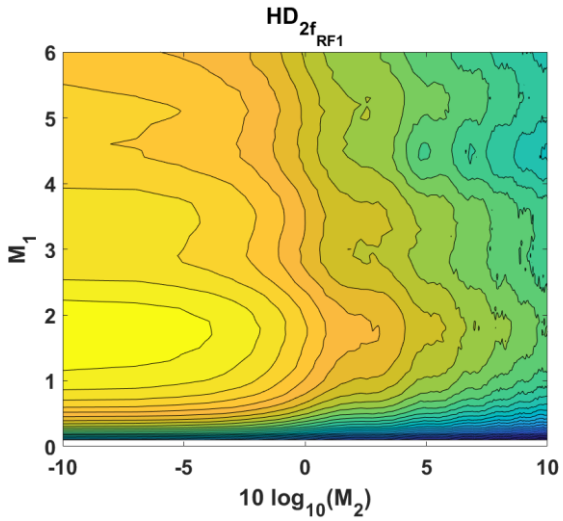

Figure 3. Simulated behavior of $HD_{2f_{RF1}}$ letting I_{RF1} and I_{RF2} to vary independently. See text for details.

3.2 Reduction of the distortion impact

Assuming for simplicity, but without loss of generality, to modulate the optical carrier with a single tone of frequency $f_{RF1} = 70MHz$, the proposed countermeasure consists in introducing an additional modulating (dithering) tone, with amplitude I_{dith} and a much lower frequency, $f_{dith} = 10KHz$, so that it does not fall inside the bandwidth considered. In this case the value of the PM index $M_{dith} = K(f_{dith})I_{dith}/f_{dith}$, exhibits values which are around three orders of magnitude higher than the values of M_1.

Fig. 4 reports the behavior of $HD_{2f_{RF1}}$ for varying values of M_1 and M_{dith}. Note that in simulating the quantities which depend on M_{dith}, an experimentally-determined correction factor was applied, related to the relatively low value of the modulating frequency f_{dith}. It can be appreciated that for a given value of M_1(that may result e.g. from a RFI tone) it is always possible to determine a value of I_{dith} which determines a reduction of $HD_{2f_{RF1}}$.
However, one important point to be considered in this case is the fact that the presence of the dithering tone may in turn determine the insurgence of an undesired spurious term $IMD_{f_{RF1}+f_{dith}}$ at the frequency $f_1 + f_{dith}$, which falls inside the bandwidth under analysis. Regarding this aspect,

the model developed allows to identify the appropriate values of I_{dith}. which determine a reduction of $HD_{2f_{RF1}}$ and maintains $IMD_{f_{RF1}+f_{dith}}$ at acceptable values. Fig. 5 reports the behavior of $IMD_{f_{RF1}+f_{dith}}$, for varying values of M_1 and M_{dith}. It can e.g. be noted that in case of $M_1 \sim 1$ to reduce both the values of $HD_{2f_{RF1}}$ and $IMD_{f_{RF1}+f_{dith}}$ it is necessary to operate with $10log_{10}(M_{dith})$ greater than around 30 (i.e. I_{dith} greater than around $0.02mA$), which is somewhat counterintuitive, but is appropriately predicted by the theoretical model presented.

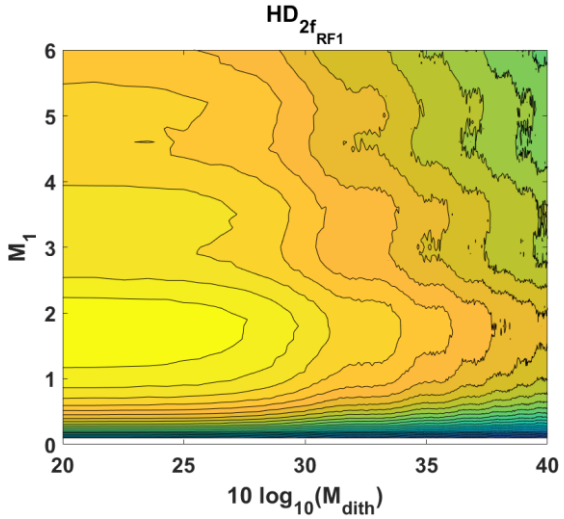

Figure 4. Simulated behavior of $HD_{2f_{RF1}}$ for varying I_{RF1} and applying a dithering tone with varying amplitudes I_{dith}. See text for details.

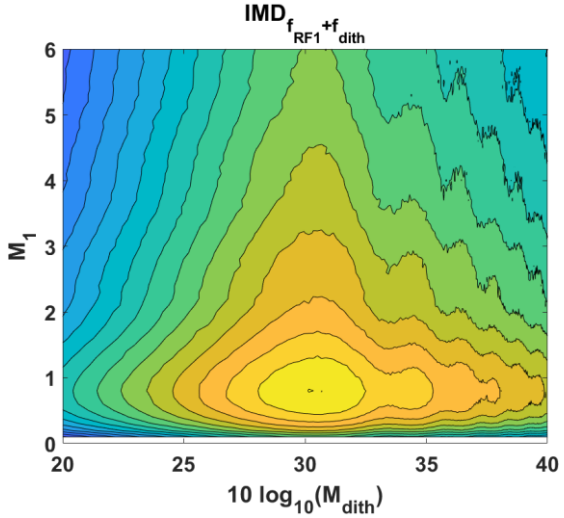

Figure 5. Simulated behavior of $IMD_{f_{RF1}+f_{dith}}$ for varying I_{RF1} and applying a dithering tone with varying amplitudes I_{dith}. See text for details.

4 Conclusions

A rigorous theoretical model which allows the study of undesired Rayleigh Backscattering-induced nonlinearities in Radio over Fiber Links has been presented and successfully validated. Its application within scenarios typical of radioastronomy allows on one side to put into evidence the beneficial reduction of such detriments through the introduction of an additional low-frequency *dithering* tone, and on the other side to identify the optimal range of values of emission amplitudes at which the corresponding oscillator has to be designed.

5 References

1. R. Beresford, W. Cheng, P. Roberts, "Low Cost RF over Fiber Distribution For Radio Astronomy Phased Arrays," *URSI GASS*, August 2017, Montreal.

2. P. Bolli et al., "From MAD to SAD: The Italian experience for the low-frequency aperture array of SKA1-LOW," *Radio Science*, **51**, March 2016, pp. 160-175.

3. M. U. Hadi et al., "Direct digital predistortion technique for the compensation of laser chirp and fiber dispersion in long haul radio over fiber links," *Optical and Quantum Electronics*, **51**, June 2019, Article number 105.

4. M. U. Hadi et al., "Linearity improvement of VCSELs based radio over fiber systems utilizing digital predistortion," *Advances in Science, Technology and Engineering Systems,* **4**, Issue 3, 2019, Pages 156-163.

5. J. Nanni et al., "Challenges due to Rayleigh Backscattering in Radio over Fibre links for the Square Kilometre Array Radio-Telescope," *ICTON*, July 2019, Angers.

6. P. K. Pepeljugoski and K. Y. Lau, "Interferometric Noise Reduction in Fiber-Optic Links by Superposition of High Frequency Modulation," *Journal of Lightwave Technology*, **vol. 10 no. 7**, July 1992.

7. S. L. Woodward and T. E. Darcie, "A Method for Reducing Multipath Interference Noise," *IEEE Photonics Technology Letters*, **vol. 6 no. 3**, March 1994.

8. J. Nanni et al., "Optimum Mitigation of distortion induced by Rayleigh Backscattering in Radio-over-Fiberlinks for the Square Kilometre Array Radio-Telescope," *MWP*, October 2019, Ottawa.

9. J. Nanni et al., "Chirp evaluation of semiconductor DFB lasers through a simple Interferometry-Based (IB) technique," *OSA Appl. Opt.,* **vol. 55**, pp. 7788-7795, August 2016.

10. P. Gysel, R. K. Staubli, "Statistical Properties of Rayleigh Backscattering in Single-Mode Fibers," *Journal of Lightwave Technology*, **vol. 8 no. 4**, April 1990.

11. B. E. A. Saleh and M. C. Teich, "Fundamentals of Photonics," John Wiley & Sons, Inc., New York, 1991.